Water in Nonpolar Confinement: From Nanotubes to Proteins and Beyond*

Jayendran C. Rasaiah,[1] Shekhar Garde,[2] and Gerhard Hummer[3]

[1]Department of Chemistry, University of Maine, Orono, Maine 04469; email: rasaiah@maine.edu

[2]The Howard P. Isermann Department of Chemical and Biological Engineering, Rensselaer Polytechnic Institute, Troy, New York 12180; email: gardes@rpi.edu

[3]Laboratory of Chemical Physics, National Institute of Diabetes and Digestive and Kidney Diseases, National Institutes of Health, Bethesda, Maryland 20892-0520; email: gerhard.hummer@nih.gov

Annu. Rev. Phys. Chem. 2008. 59:713–40

First published online as a Review in Advance on December 19, 2007

The *Annual Review of Physical Chemistry* is online at http://physchem.annualreviews.org

This article's doi: 10.1146/annurev.physchem.59.032607.093815

0066-426X/08/0505-0713$20.00

Key Words

nanofluidics, nanopores, hydrophobic effect, nanoscale drying transitions, protein hydration, proton transfer, confined fluids

Abstract

Water molecules confined to nonpolar pores and cavities of nanoscopic dimensions exhibit highly unusual properties. Water filling is strongly cooperative, with the possible coexistence of filled and empty states and sensitivity to small perturbations of the pore polarity and solvent conditions. Confined water molecules form tightly hydrogen-bonded wires or clusters. The weak attractions to the confining wall, combined with strong interactions between water molecules, permit exceptionally rapid water flow, exceeding expectations from macroscopic hydrodynamics by several orders of magnitude. The proton mobility along 1D water wires also substantially exceeds that in the bulk. Proteins appear to exploit these unusual properties of confined water in their biological function (e.g., to ensure rapid water flow in aquaporins or to gate proton flow in proton pumps and enzymes). The unusual properties of water in nonpolar confinement are also relevant to the design of novel nanofluidic and molecular separation devices or fuel cells.

INTRODUCTION

"Oil and water do not mix." This everyday observation is the quintessential hydrophobic effect. At the molecular level, hydrophobic effects are thought to drive a variety of biological and colloidal self-assembly phenomena in aqueous solution, including the folding of proteins and the formation of micelles and membranes. Naturally, investigators have focused much attention on the hydration thermodynamics of nonpolar molecules in water and their water-mediated hydrophobic interactions. In essence, those studies show that small hydrophobic solutes are insoluble in water primarily because of a large entropic penalty commonly associated with a perturbation of the vicinal water structure. Such descriptions, however, tell only half the story.

Much less studied is the other half: the low solubility of water in oil. Wolfenden & Radzicka (1) found that the equilibrium concentration of water in nonpolar solvents is indeed low, making them literally hydrophobic. For the transfer of water from vapor into cyclohexane and heptane, the equilibrium constant is approximately one at ambient conditions, corresponding to a water concentration of $\sim 10^{-3}$ mol per liter, or approximately one water molecule per 1000 nm^3. Clearly, this low solubility originates from the lack of strong attractive interactions between water and the nonpolar molecules. Furthermore, the relative lack of free volume formed through transient density fluctuations in nonpolar solvents (2) keeps the water concentration almost as low as that in vapor.

Would water occupy nonpolar molecule-size cavities if they were preformed, instead of being formed transiently? Answers from experiments are far from conclusive. The well-defined structures of folded proteins contain cavities, caused by packing imperfections or engineered by site-directed mutagenesis. Researchers have studied the hydration of the protein interior in great detail (3–13). Remarkably, there is no general consensus regarding whether typical nonpolar cavities inside proteins are water filled or empty, and even in specific cases the results of different experimental probes diverge (4, 6, 8).

From a fundamental perspective, water is expected to recede from nonpolar interfaces and cavities. Invoking the contact theorem of statistical mechanics, Stillinger (14) argued more than 30 years ago that a liquid water phase at ambient conditions does not wet a hard wall, but instead forms a water-vapor interface near the wall. Recent theoretical developments (15) and related simulation studies (16, 17) span the length-scale-dependent hydration of hard-sphere solutes from molecular to macroscopic sizes (18). Water molecules pack well near small solutes, thus wetting the interface; with increasing solute size, water dewets hard-solute surfaces. This crossover from wet to dry interfaces begins at subnanometer length scales.

For the concave surface of a pore or cavity, such drying effects should become even more pronounced, with water molecules subjected to an effective cavity expulsion (19) owing to the lack of hydrogen-bonding interactions with the confining volume. Indeed, computer simulations by Wallqvist & Berne (20) showed such drying between ellipsoidal purely repulsive plates. However, realistic systems exert attractive van der Waals and polarizability-induced interactions with water. These weak attractions can

become strong enough such that a low-order perturbative treatment must include the coexistence of both dry and wet states to adequately describe the system (21, 22).

The question of water in nonpolar confinement is not only of academic interest. In many proteins, nonpolar cavities are often located at or near the active site and are thought to be involved in the uptake, transfer, and release of both nonpolar and polar molecules. In particular, nonpolar or weakly polar pores play a prominent role in aquaporin water channels, the biological proton pumps cytochrome *c* oxidase and bacteriorhodopsin (23), cytochrome P450 (24, 25), and the gating region of potassium channels (26, 27). In all these systems, evidence is accumulating that water occupies their weakly polar pores at least transiently.

The penetration of water into nonpolar pores is also of technological relevance, in part building on the rapid advances in nanoscale synthesis. Initial computer simulations (21, 28, 29) and subsequent experiments (30, 31) suggest that water can flow through hydrophobic nanopores with greatly reduced wall friction, exceeding flow rates predicted by the macroscopic Hagen-Poiseuille law by three to four orders of magnitude. Combined with chemical selectivity (32, 33), such as ion exclusion from the pores (28), the possibility emerges of building efficient molecular separation devices (34), and maybe even novel desalination technology (28, 35), based on materials with nanoscopic nonpolar pores. Lastly, if the challenge of low proton density in nonpolar pores can be solved (36), the single-file hydrogen-bonded water wires in highly confined nanopores (**Figure 1**) would form ideal proton conduction wires (36–39), with potential applications in fuel cells, for instance (36, 40).

Here we review recent efforts to quantify the thermodynamics of water filling nonpolar or weakly polar pores and confinements [including those in carbon nanotubes (CNTs), fullerenes, and proteins] and characterize the unique properties of water in such nonpolar confinements. We then discuss the implications of these results on the function of biomolecular systems and possible applications.

THERMODYNAMICS, STRUCTURE, AND KINETICS OF WATER FILLING NONPOLAR PORES AND CAVITIES

Theory

If particle exchange between the cavity and the bulk solvent is not fast on the simulation timescale, one can establish a virtual particle equilibrium using a grand-canonical formalism. We consider a probe volume V covering a cavity of interest in a molecular system embedded within a larger volume V' in a canonical ensemble at temperature T. The subvolume V is in thermal equilibrium with the surrounding, and in chemical equilibrium with a water bath at a total chemical potential μ. The probability of observing exactly N particles in the volume V is then given by

$$P(N) = \frac{z^N}{\Xi N!} \int d\mathbf{s}^M \int_V d\mathbf{r}^N e^{-\beta U_N(\mathbf{r}^N, \mathbf{s}^M)}, \quad (1)$$

where $\Xi = 1/P(0)$ is the (semi-)grand partition function ensuring normalization, $\sum_{N=0}^{\infty} P(N) = 1$. U_N is the configurational energy of N particles at positions $\mathbf{r}^N$

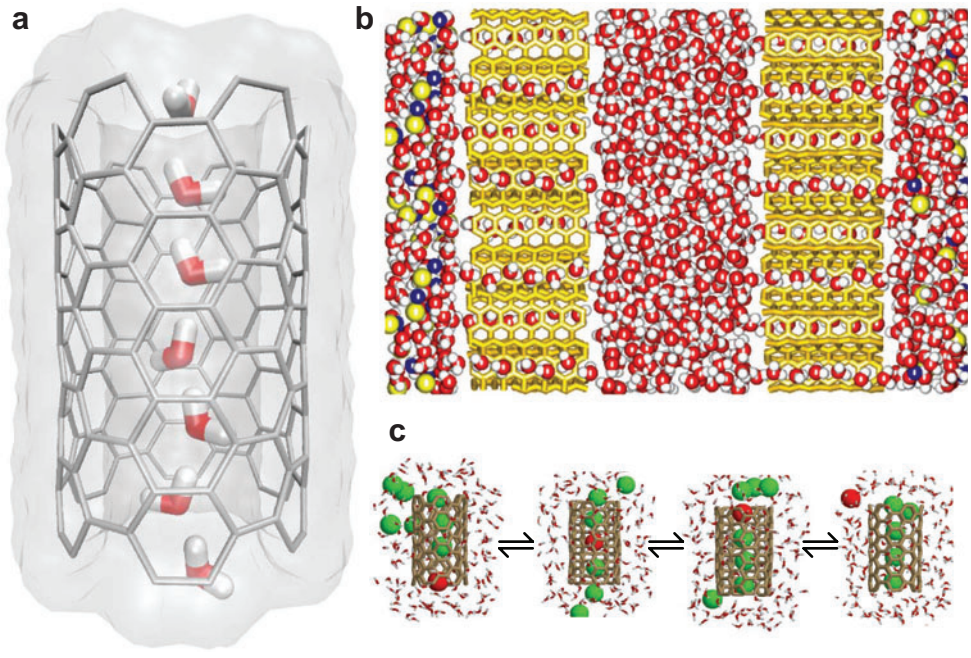

Figure 1

Carbon nanotubes (CNTs) as molecular channels for water and solutes. (*a*) Snapshot of a 1D hydrogen-bonded water wire in the pore of a short (6,6) CNT immersed in water (21). (*b*) Osmotically driven flow from a pure-water compartment (*center*) through two CNT membranes (*gold*) into a salt-solution compartment (*left and right*; connected by periodic boundary conditions) (28). (*c*) Selective partitioning of methane molecules (*green spheres*, plus one tagged *red sphere*) and transport through a CNT immersed in water (33).

in volume V, which contains interactions with M other particles at positions $\mathbf{s}^M$, including solvent molecules outside V, and possibly an external potential such as a cavity wall. $z = \rho e^{\beta\mu^{\rm ex}_{\rm bulk}}$ is the activity of the particles in V; ρ is the number density of the bulk phase with which they are in equilibrium; and $\mu^{\rm ex}_{\rm bulk}$ is the corresponding excess chemical potential, with $\beta = 1/k_BT$ and k_B as Boltzmann's constant. We can then write the ratio of probabilities that the volume contains $N+1$ and N molecules, respectively, as

$$\frac{P(N+1)}{P(N)} = \frac{\rho V e^{\beta\mu^{\rm ex}_{\rm bulk}}}{N+1}\left\langle e^{-\beta(U_{N+1}-U_N)}\right\rangle_N, \qquad (2)$$

where $\langle e^{-\beta(U_{N+1}-U_N)}\rangle_N \equiv \exp(-\beta\mu^{\rm ex}_N)$ is a canonical test-particle average of the binding energy of an $(N+1)$-th water molecule randomly inserted into the cavity containing N water molecules. This average defines the excess chemical potential $\mu^{\rm ex}_N$ for a state with N water molecules confined to V. In computer simulations, one can calculate the average, for instance, by test-particle insertion, or Bennett's (41) method of overlapping histograms from the normalized distributions $p_{{\rm ins},N}(\Delta U)$ and

$p_{\mathrm{rem},N+1}(\Delta U)$ of particle insertion and particle removal energies $\Delta U = U_{N+1} - U_N$, respectively:

$$\frac{p_{\mathrm{ins},N}(\Delta U)}{p_{\mathrm{rem},N+1}(\Delta U)} = e^{\beta\Delta U}\left\langle e^{-\beta(U_{N+1}-U_N)}\right\rangle_N. \quad (3)$$

In a plot of $\ln p_{\mathrm{ins},N}/p_{\mathrm{rem},N+1}$ against ΔU, the slope should be β, and the intercept with $\Delta U = 0$ gives the excess chemical potential of the confined water, $-\beta\mu_N^{\mathrm{ex}} = \ln\langle\exp[-\beta(U_{N+1}-U_N)]\rangle_N$. Equation 3 thus allows one not only to calculate the excess chemical potential of the confined water μ_N^{ex}, but also to test whether the confined water is in proper thermal and chemical equilibrium.

The procedure involves performing a series of simulations with different occupancies $N = 1, 2, \ldots, N_{\max}$ and combining the insertion and removal energy distributions from simulations with N and $N+1$ particles, respectively, to estimate $\langle e^{-\beta(U_{N+1}-U_N)}\rangle_N$ via Equation 3. Recursive application of Equation 2 then gives $P(N)/P(0)$ for $N \geq 1$, and finally, $P(0) = \Xi^{-1}$ is found by normalization (22, 42). The resulting average water occupancy $\langle N\rangle$ is related to the differences in the excess chemical potentials of water in the interior (cavity) and exterior (bulk). From Equation 2, we find that $\langle N\rangle = \sum_N NP(N) = \rho V e^{-\beta(\mu^{\mathrm{ex}}-\mu^{\mathrm{ex}}_{\mathrm{bulk}})}$, where $\exp(-\beta\mu^{\mathrm{ex}}) = \sum_N P(N)\exp(-\beta\mu_N^{\mathrm{ex}})$ is the average excess chemical potential of water in the cavity (42).

We can also discuss the thermodynamics of confined water in terms of the free energy of transfer from an external water reservoir. We rewrite Equation 1 as $P(N) = \Xi^{-1}\exp(\beta\mu N - \beta A_N)$, where A_N is the Helmholtz free energy of the system with N water molecules in V (42) and μ is the total chemical potential of the bulk fluid. Because $P(0) = \Xi^{-1}$, A_N can be determined from the ratio of probabilities in filled and empty states. The Helmholtz free energy of N water molecules in the bulk fluid is $A_{N,\mathrm{bulk}} = \mu N - pV_{N,\mathrm{bulk}}$, where p is the pressure and $V_{N,\mathrm{bulk}}$ is the volume of N water molecules in the bulk phase.

Through Equation 1 and $P(0) = \Xi^{-1}$, the free energy ΔA_N of the transfer of exactly N water molecules from the bulk phase into the probe volume V is related to the occupancy probabilities $P(N)$ by $\Delta A_N = A_N - A_{N,\mathrm{bulk}} = -k_B T\ln P(N)/P(0) + pV_{N,\mathrm{bulk}}$. Near ambient conditions, the pressure-volume term is small, $pV_{N,\mathrm{bulk}}/N \approx 0.002$ kJ mol^{-1} (22, 42), and can be neglected. From the temperature dependence of $\Delta A_N = \Delta U_N - T\Delta S_N$, we can estimate the internal energy ΔU_N and entropy $\Delta S_N = -\partial\Delta A_N/\partial T$ of water in the confined system relative to bulk water. We note in particular that if (for a given occupancy N) the energy and entropy of transfer are essentially constant over a small temperature range, a plot of $-N^{-1}\ln[P(N)/P(0)]$ versus T^{-1} furnishes $\Delta U_N/N$ and $\Delta S_N/N$ from the slope and intercept, respectively. For protein cavities, an approximate procedure has been used to estimate the energy of transfer (43). If the cavity is relatively rigid, such that protein and solvent reorganization energies are small, then the energy difference can be approximated as $\Delta U_N/N \approx \langle U_{\mathrm{rem}}\rangle_N/N - \langle U_{\mathrm{rem}}\rangle_{\mathrm{bulk}}/2$, where $\langle U_{\mathrm{rem}}\rangle_N$ is the average removal energy of the entire N water cluster from the cavity, and $\langle U_{\mathrm{rem}}\rangle_{\mathrm{bulk}}/2 = \langle U\rangle_{\mathrm{bulk}}$ is half the removal energy for bulk water, which corresponds to the average total energy per particle.

A global free-energy minimum at a nonzero occupancy $N > 0$ implies that filling is favored at that occupancy. In this case, a free-energy barrier usually exists between the

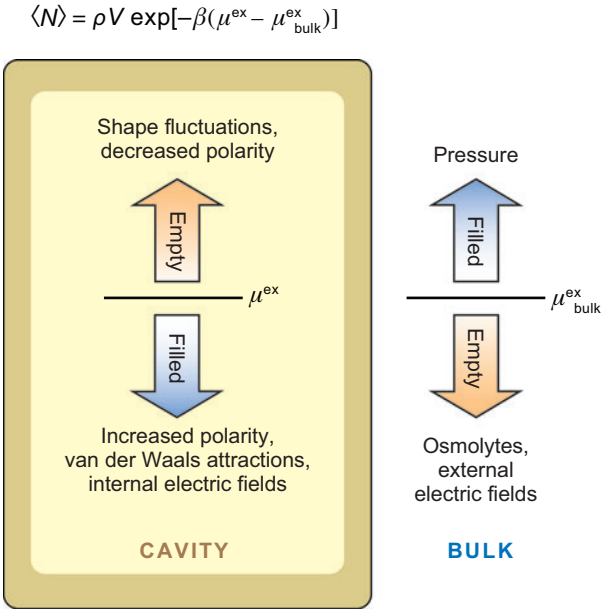

Figure 2

Thermodynamics of water filling a cavity. The amount of water in a cavity is governed by the difference between the excess chemical potential inside and in the bulk. This difference is sensitive to changes in internal factors (such as the polarity of the cavity, van der Waals attractions, internal electric fields, and shape fluctuations), as well as external factors acting on the bulk phase (such as pressure, osmolyte concentration, or external electric fields).

occupied and empty states; the barrier partially controls the kinetics of emptying and filling. Additional factors that determine the kinetics are frictional resistance along the reaction path and end effects such as density fluctuations and energy barriers near the entrance to the cavity or CNT (44). When the free energy of transfer to filled states is near zero and an easily accessible low-friction path exists between the states, the system fluctuates between empty and filled states over timescales governed by the barrier and temperature (45).

Factors Controlling the Thermodynamics of Filling

A number of factors determine the difference in excess chemical potential of water inside and outside a cavity. Filling can be achieved by making either the excess chemical potential in the cavity interior favorable or the outside unfavorable (**Figure 2**).

Attractive interactions and local polarity. Simulations of a narrow CNT (~0.8-nm diameter) immersed in water showed that a small reduction of the van der Waals attraction between water and the carbon atoms induces drying of the previously water-filled pore (21, 45). Sensitivity of the water occupancy to changes in the geometry and interaction energy with the surrounding medium was observed also for other systems (46–58). The water contact angle with graphitic surfaces was similarly found to be sensitive to graphite-water interactions (59).

Figure 3 illustrates the drying of a solvated CNT upon weakening the carbon-water attractive interactions. The depth of carbon-water pair interaction potentials differs by only approximately 0.05 kcal mol^{-1} (less than 0.1 k_BT) in the two cases.

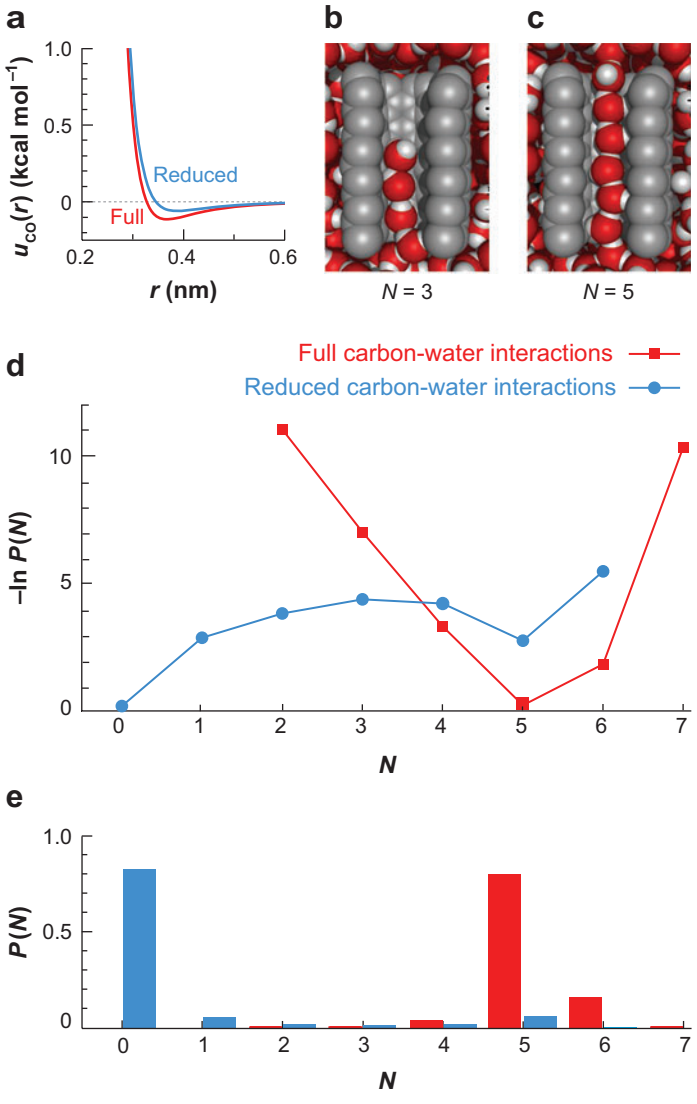

Figure 3

Emptying transition of a solvated carbon nanotube (CNT) (21). (*a*) Full and reduced carbon-water pair potential. (*b*, *c*) Snapshots of a CNT partially and fully filled with water. (*d*) Free energy of occupancy fluctuations, $\beta F(N) = -\ln P(N)$, as a function of the occupancy N.

In contrast, the probability $P(N)$ of finding exactly N water molecules inside the tube is significantly different. It is sharply centered around the fully filled state ($N = 5$) for a system with full-strength carbon-water interactions and becomes bimodal when attractions are reduced. The free energy of occupancy fluctuations, $F(N) = -k_B T \ln P(N)$, shown in **Figure 3** highlights the difference clearly.

The weakened carbon-water attractions primarily increase the excess chemical potential of water inside the nanotube. As the excess chemical potential of the confined water approaches that of bulk water, and eventually exceeds it, the system could respond in two ways. In a gas-like response, the confined water would simply dilute,

resulting in fragmentation of the hydrogen-bonded water wire. Alternatively, in a liquid-like response, the system would separate into a gas-like essentially empty state and a liquid-like filled state. On a microscopic scale, the two phases cannot coexist. Instead the system fluctuates between a water-filled and empty state. A relatively high free-energy barrier between the two states reflects the high energetic cost of fragmented hydrogen bonds and ensures that the transitions are two-state-like (21, 45).

This sensitivity highlights the challenge of making quantitative predictions with molecular force fields that neglect, for example, polarizability effects, or the specific chemistry at the CNT rims. Nevertheless, important qualitative trends, such as the cooperative drying of pores upon weakening the attractions, should be properly captured, and accurate predictions of drying thermodynamics have been made (9).

Solvent conditions: temperature, pressure, osmolyte concentration. The filling equilibrium can also be affected by changing the excess chemical potential of water on the outside, for example, by applying pressure or adding salts or osmolytes that do not penetrate the tube. For a structurally pressure-stable cavity, the excess chemical potential inside is barely affected by pressure; outside, however, pressure increases the chemical potential according to $(\partial\mu/\partial p)_T = 1/\rho$. For bulk water, a pressure increase to 1 kbar (100 MPa) raises the total chemical potential by approximately 2 kJ mol^{-1}, a change that can be sufficient to tilt the balance from a previously empty toward a filled state. Experiment and simulation demonstrated such water filling for a nonpolar cavity inside the L99A mutant of the protein T4 lysozyme (**Figure 4**) (9, 60).

Interestingly, temperature appears to have only a modest effect on the water occupancy of nonpolar cavities. We probed the temperature-dependent occupancy of CNT pores (42), fullerenes, and simple spherical cavities (22), as well as that of cavities in proteins by molecular simulations. The entropy of transferring water from the bulk into the channel of narrow CNTs (**Figure 1*a***) was near zero even in the completely filled state (42), reflecting that water in 1D wires retains considerable rotational entropy, with a dangling hydrogen able to rotate about the water-wire axis. However, we note that the thermodynamics of transfer differs for isolated tubes and tubes open to a bulk-water reservoir. In open, partially filled tubes, water molecules typically remain hydrogen bonded to the external solvent, thereby lowering both their energy and entropy (42a; A. Waghe, unpublished manuscript).

For water in spherical pores, the entropy of transfer was found to be negative for the filled state (22). We obtained similar results for the nonpolar cavities of the protein tetrabrachion (43) (**Figure 5*c***). Dunitz (61), based on the entropies of hydration water in crystals and in bulk, argued for slightly unfavorable entropies of water in protein cavities. Denisov et al. (62), based on nuclear-magnetic-resonance data and a model for librational motion, suggested that the entropy of water transfer into less polar cavities may even be positive (i.e., favorable). Collectively, the above arguments and simulation data suggest that temperature has only a modest influence on the water occupancy in a narrow CNT pore, but favors the empty states of spherical-shape nonpolar cavities, and in proteins.

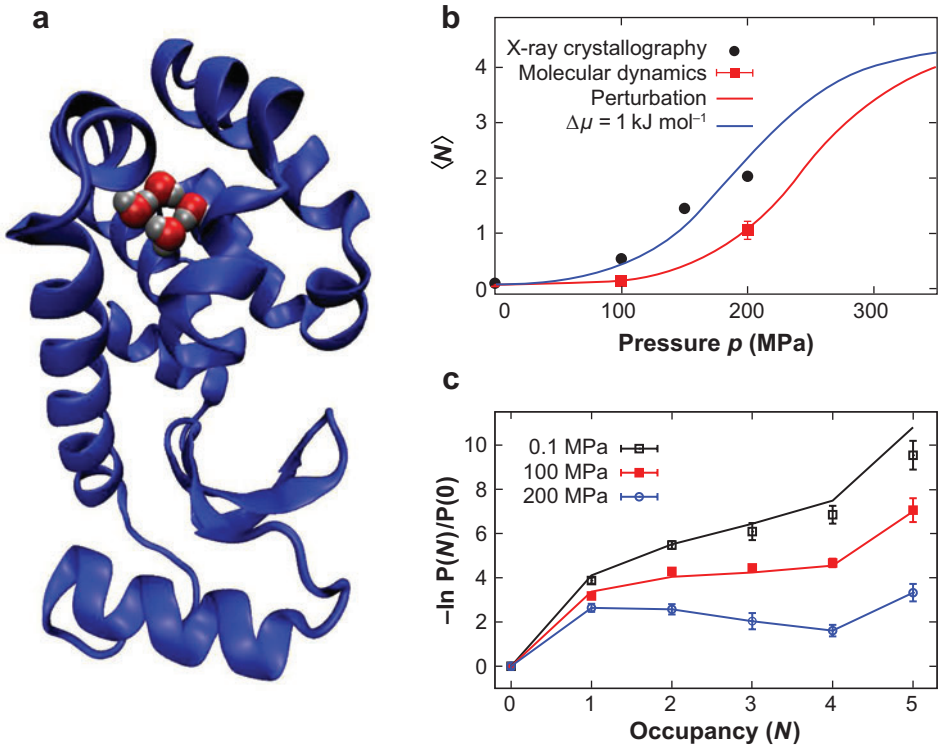

Figure 4

Water penetration into a hydrophobic cavity in the L99A mutant of T4 lysozyme (9, 60). (*a*) Snapshot of a square-type four-water cluster in the cavity, shown with the protein backbone. (*b*) Average occupancy of the cavity as a function of pressure, comparing results from high-pressure X-ray crystallography [*filled circles*, obtained by integrating the electron density in the cavity (9)] to molecular dynamics simulations (*red squares*). Perturbation theory using the 200-MPa state as a reference gives the red line. A small shift ($\Delta\mu = 1$ kJ mol^{-1}) in the bulk chemical potential of the water model (*blue curve*) brings the simulation results into quantitative agreement with experiment. (*c*) Free energy of transfer, $-\ln[P(N)/P(0)]$.

Electric field. The effect of electric fields on water permeation though nanopores was studied in simulations (42, 63–65). Dzubiella et al. (63) showed that water permeation can be controlled and enhanced by electric fields. Vaitheeswaran et al. (42) found that an electric field along the axis of a narrow CNT favors filling and orients the water dipoles in the tube in the direction of the field, with the field effects described nearly quantitatively by a model with only two dipolar states (collectively pointing up or down) and two filling states (empty or filled).

Electric fields can also have more complicated effects on confined water. Zimmerli et al. (66) found that local electric fields perturbed both the dipolar orientation and the filling of CNTs. Li et al. (64) showed that the electric field of a charge localized near a narrow CNT leads to increased ordering of the water along the pore axis,

Figure 5

Solvation of protein cavities. (*a*) A nine-water cluster in the large interior cavity of the protein tetrabrachion (43). Part of the cavity surface is shown in dark blue. (*b*) A nine-water cluster inside the fullerene C_{180}, which has a cavity size comparable to that in tetrabrachion (22). (*c*) The thermodynamics of water transfer into the large cavity of tetrabrachion (43).

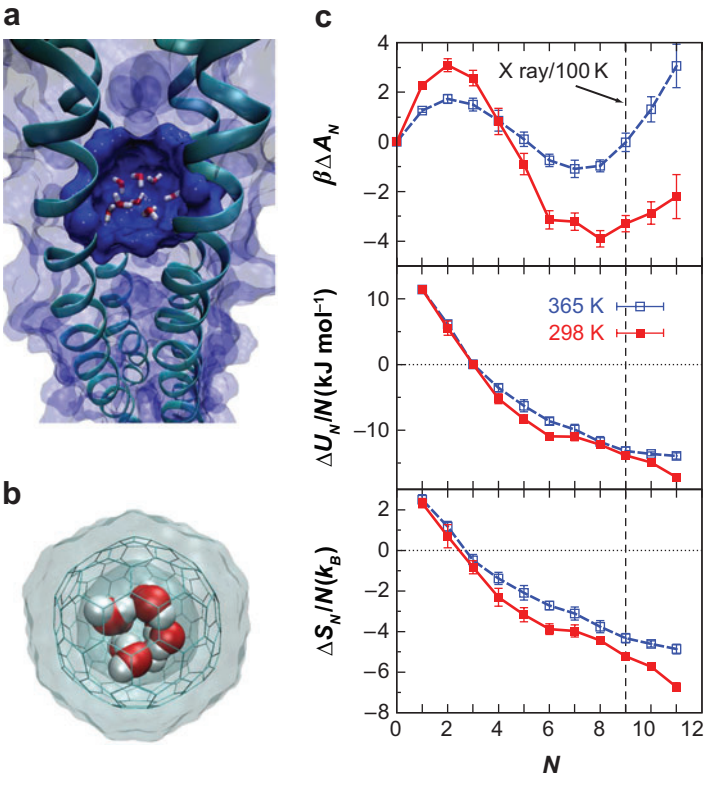

thereby reducing the rate of water transport across the pore. In simulations of proton transport along ordered water chains, Hassan et al. (38) found that local electric fields either enhance the proton transfer rate or slow it down, depending on the field strength and the resulting perturbation of the water structure and electrostatics. Even the presence of ions in solution localized near the pore was found to affect the structure and dynamics of water inside (63, 65). Sufficiently large electric fields applied between small graphene sheets in water were shown to induce drying instead of causing the increase in the water density expected from linear polarization response at low fields (53). However, simulations of water in nanopores have also shown conventional electrostriction in contrast to the above result (67).

Conformational flexibility. Changes in the conformational flexibility can also affect the equilibrium between filled and empty states. As Andreev et al. (68) demonstrated using computer simulations, water was effectively squeezed out of a small CNT in water that was artificially made more flexible. The main effect appeared to be a reduction in the free volume of the confined water molecules, which are thereby forced into an energetically less favorable straight arrangement. Moreover, in the water-filled state, low-frequency modes of the tube are suppressed. Both effects help shift the equilibrium toward the empty state. In the case of proteins, simulations by

Damjanović et al. (69) also suggested that flexible, small, nonpolar cavities tend to be empty.

Structure of Water in Nonpolar Confinement

Subnanometer confinement strongly affects the molecular properties of fluids (21, 70–73) and, in particular, their structure. For water in nonpolar confinement, a main factor is the formation of strong hydrogen bonds (21, 72, 74, 150).

Spherical pores. The almost-spherical and nonpolar internal cavities of fullerenes (C_{140} and C_{180}) have sufficient space to accommodate hydrogen-bonded clusters of several water molecules (22). For graphene-like cavity-water interactions, the free energy of transfer of water from a reservoir into a cavity displays two-state behavior, with minima at $N = 0$ (empty/dry) and $N > 0$ (filled), when the cavity diameter exceeds ~1 nm. Smaller cavities remain empty at room temperature and pressure. Reducing the cavity-water attraction leads to drying of cavities in equilibrium with bulk water for all cavity sizes. However, Iwamatsu et al. (75) demonstrated in their experiments using toluene-water mixtures that even the small cavity of an open-cage C_{60} derivative could be filled by water, reflecting an increased chemical potential of water on the outside.

As the occupancy of a cavity increases, the formation of water-water hydrogen bonds decreases the system enthalpy. Cavity-water attraction provides essentially a mean field contribution that lowers the enthalpy. In contrast, the entropy of transfer is favorable (positive) for low occupancies and gradually becomes less favorable with rising occupancy, reflecting hydrogen-bond formation and loss of free volume.

The structures of encapsulated water clusters (**Figure 5*b***) shed light on the origin of their thermodynamic stability. The smallest marginally stable cluster, observed in simulations of a cavity of 1.0-nm diameter, has three water molecules hydrogen bonded in a triangle configuration (22). As the diameter increases, cyclic structures evolve from trimers to hexamers, with each water molecule donating and accepting a hydrogen bond. In a pentamer, the fifth water oxygen moves out of the plane of the other four oxygen atoms to relieve the ring strain. The water hexamer shows coexistence between ring- and cage-like structures. Interestingly, the properties of some highly structured water clusters in the simulations are similar to those found experimentally in the gas phase (76). Cavity encapsulation may thus provide a means to study the properties of water clusters, especially when they are unstable or not easily prepared in an unconfined state. Differences in structural details motivate simulations with better water models (22, 77).

Cylindrical pores. Open-ended CNTs and other cylindrical nanopores allow easy access for solvent water molecules and can be filled under appropriate thermodynamic or solution conditions, as shown not only by simulation (21) but also by electron microscopy (78), X-ray and neutron scattering (79, 80), light spectroscopy (81), and nuclear-magnetic-resonance spectroscopy (82–84). Water filling of CNTs had indeed been predicted based on the macroscopic surface tension (85). The water structure

in the well-defined confinement of CNTs displays a remarkable diversity depending on pore size, temperature, and pressure. In tubes having small yet fillable internal pore diameters [e.g., (5,5) or (6,6) CNTs], water molecules form single-file hydrogen-bonded (typically unidirectional) wires (21) (see also the discussion of proton transport and aquaporin, below). As the tube diameter is increased, more water molecules access the interior, and increasingly more complex layered structures emerge. At ambient or higher temperatures, the confined water is in a liquid phase, in which thermal fluctuations coarse grain water's tendency to form specific many-body hydrogen-bonded structures. Lowering the temperature (in the range of 280–260 K), however, leads to solidification and new and interesting phases of high-density ice, as seen in computer simulations (86) and experiments (79, 83). These quasi-1D crystalline ice phases are characterized by stacking of n-membered rings in the axial direction (n = 4–7, with increasing tube diameter from 1.1 to 1.4 nm). Water molecules in these rings typically satisfy ice rules with each water molecule being a double donor and acceptor of hydrogen bonds (87). The presence of a defect can lead to interesting helical structures in the tube.

Transition to and the thermodynamic stability of the quasi-1D ice phases are also fundamentally interesting. For example, the transition from square liquid-disordered to crystalline-ordered ice phases ($n = 4$) upon cooling in (14,14) CNTs is continuous, whereas the liquid to hexagonal-ring stacked ice phase transition in a (16,16) tube is discontinuous first-order-like (86, 88). Systematic exploration of the pressure-temperature space for transitions in (14,14) CNTs indicates the presence of a solid-liquid critical point (86), which is absent in the bulk water phase. A more recent extension of these studies to pressures exceeding 1 GPa indicates the formation of helical multiwalled ice phases in CNTs (89) (**Figure 6**). These studies bring out the remarkable ability of water molecules to adapt to nanoscopic confinements by forming hydrogen-bonded arrangements that are essentially absent in bulk. However, ordered structures inside CNTs are not unique to water. For instance, 1D ionic crystals in equilibrium with a disordered solution phase have been reported (90, 91).

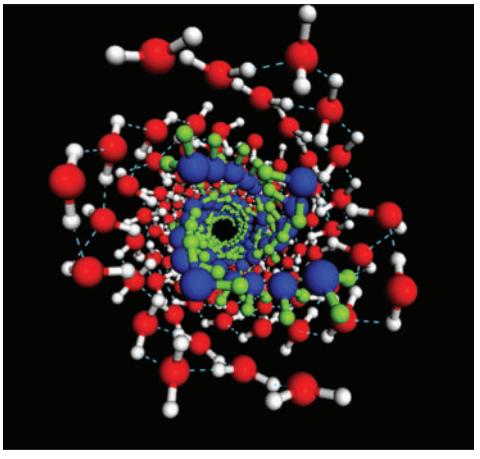

Figure 6

Ice helix in a (17,0) CNT at 4-GPa pressure (89). Figure courtesy of X.C. Zeng. Copyright (2006) the National Academy of Sciences, U.S.A.

Water between plates. Theory and simulations indicate drying between strongly hydrophobic plates in water separated by a few nanometers or less (15, 52). However, under conditions that permit water filling of the space between plates (i.e., if the plates are sufficiently polar or for certain bulk solvent conditions), unique water structures in planar confinement were observed in simulations. For example, for water sandwiched between CNT membranes at molecular separations (28), a water monolayer was found to be in equilibrium with the bulk phase. The resulting water structure is templated by the membrane surfaces and clearly shows meshed inner 6-membered and outer 12-membered ring-like arrangements even at 300 K. Another recent study shows that water between hydrophobic plates separated by 6 Å can freeze into a bilayer ice crystalline phase at 300 K and pressures above 0.1 GPa (92). No such freezing was observed when the plates were hydrophilic, indicating the importance of water-water hydrogen-bonding interactions in hydrophobic confinements.

Water in Protein Cavities

Although tightly packed overall, many folded proteins contain a number of interior cavities or pores large enough to hold water or other small molecules. These cavities can serve as functionally relevant access channels or binding sites for substrates or products. Interestingly, a number of internal cavities are lined with predominantly nonpolar groups, and the experimental results for the hydration of such cavities are not entirely clear. X-ray crystallography often finds nonpolar cavities to be empty (3, 8), with some exceptions (6, 93); in contrast, nuclear-magnetic-resonance spectroscopy has provided evidence for the presence of water in weakly polar cavities (4, 5). On the theoretical side, a large number of studies using, for example, energetic estimates (94), molecular simulations (95–97), and statistical-mechanical theory (98, 99) have explored the hydration of proteins and nucleic acids. In many interesting cases of larger cavities, occupancy by multiple water molecules presents a challenge, making entropic considerations relevant and requiring formalisms as described above.

Lysozyme. High-pressure X-ray crystallography combined with molecular simulations (9, 60) permitted the first direct experimental observation of a molecular drying transition. For the L99A mutant of T4 lysozyme, high-pressure experiments showed that the overall structure of the protein changed minimally over the pressure range of 0–200 MPa, even around a cavity large enough to hold approximately five water molecules. At ambient pressure, the cavity was found to be empty based on the absence of appreciable electron density. However, above pressures of ~1 kbar (100 MPa), the electron density increased sharply with pressure (**Figure 4*b***), indicating a cooperative water-filling transition. Indeed, molecular dynamics simulations using the above methodology (9, 60) supported such a filling transition (**Figure 4*c***). The simulations agreed quantitatively with the integrated electron density as a function of pressure after only a small correction (by 1 kJ mol^{-1} or 0.4 k_BT) in the bulk water chemical potential of the water model (**Figure 4*b***). Simulations also provide additional structural details on water in the cavity. Specifically, a cluster of four water molecules with tight intracluster hydrogen bonds was observed (**Figure 4*a***). Finally, the molecular dynamics simulations also gave evidence for the water access and exit pathway.

Exit events from different filling states were found to take the same path through the protein, involving the transient opening of a gate formed by a phenylalanine side chain. Interestingly, and consistent with this observation, the phenylalanine side chain showed considerably larger conformational motion in the crystal than other phenylalanines, as measured by its crystallographic B factor (9, 60).

Tetrabrachion. Arguably the largest nonpolar protein cavity discovered so far is located inside tetrabrachion (100). The cavity is large enough to hold nine water molecules (**Figure 5**) and was found to be completely filled in a low-temperature (100 K) X-ray structure (100). Tetrabrachion is unusual in other ways: It remains stable at high temperatures, requiring extreme conditions for denaturation (6 mol per liter guanidine at 130°C) (101). The right-handed coiled-coiled structure of this unusual protein has additional cavities, connected by a narrow central channel along its axis (100). Simulations employing the above formalism (43) explored whether the confined water is thermodynamically stable at ambient conditions and the temperature of optimal growth of the thermophilic organism, 365 K (92°C); if the cavity dries before the protein denatures; and what possible functional role those large nonpolar cavities might play.

The free-energy profiles as a function of the occupancy (**Figure 5*c***) have two minima, corresponding to the empty state, $N = 0$, and the filled state containing between 6 and 10 water molecules (**Figure 5*a***). At 298 and 365 K, the free energy of transfer to the filled state is negative, and the cavity remains preferentially filled rather than empty. The transfer of one or two water molecules is unfavorable despite the presence of carbonyl oxygen atoms in the cavity walls as hydrogen-bonding sites and the large size of the cavity. The most probable occupancy numbers ($N = 7$ and 8 at 365 and 298 K, respectively) are in agreement with experiment ($N = 9$ at 100 K). Similar agreement was found for the smaller cavity filled by five water molecules (43).

The energy and entropy of transfer of one and two water molecules from the bulk phase into the cavity are positive but decrease with increasing occupancy to become negative beyond $N = 3$ (**Figure 5**). This decrease reflects energy-entropy compensation associated with hydrogen-bond formation in a connected water cluster.

One can infer the temperature at which the cavity dries from the calculated transfer energies and entropies, which are nearly independent of temperature. Remarkably, this drying temperature of ~384 K is just above the temperature of optimal growth (365 K) and well below the unfolding temperature. At the optimal-growth temperature, the cavity thus may be near the coexistence of filled and empty states. As a possible functional role, the cavity might be involved in the hydrophobic anchoring of a protease to tetrabrachion (43), which was shown to be attached on top of the cavity site at temperatures up to ~120°C (101).

Alzheimer's Aβ amyloids. Interestingly, quasi-1D water wires have also been seen in simulations of Alzheimer's Aβ amyloid fibrils (102, 103), one in a predominantly nonpolar pore along the fibril axis and the other in a mixed polar/nonpolar pore facing an interior salt bridge. However, at present their biological relevance is not clear.

MOLECULAR FLOW THROUGH NONPOLAR NANOPORES

Water Flow

Molecular pores that communicate with fluid reservoirs form possible conduits for nanoscale fluid flows. In biological systems, aquaporin proteins (104–111) mediate the flow of water across lipid membranes. At their narrowest region, these channels are just wide enough for water molecules to pass through, thereby providing size selectivity, but also imposing single-file motions. Interestingly, a significant fraction of the pore surface was found to be only weakly polar (104–106).

CNTs provide simple model systems to explore nanoscale hydrodynamic flows and their molecular characteristics. In a simulation of a narrow CNT immersed in water, we observed a burst-like flow of water across the pore (21). The stochastic character of the flow could be described quantitatively in terms of a continuous-time random walk (29, 44) in which the water chain spanning the pore makes collective back-and-forth motions, thereby randomly releasing water molecules on one side and picking up new ones on the other. Averaged over time, such an unbiased random walk does not lead to any net flow.

Zhu et al. (112) simulated flow in an asymmetric environment by applying a pressure gradient across a membrane channel. To study osmotically driven flow, as in biological systems, Kalra et al. (28) constructed water-permeable membranes by packing short and narrow CNTs into a 2D hexagonal array (**Figure 1*b***). Under 3D periodic boundary conditions, two such membranes divide the simulation cell into two separate solvent compartments (113), one of them filled with pure water, the other with a concentrated salt solution. The (6,6) CNTs (~0.8-nm diameter) were too narrow for ion passage (27, 28). The resulting osmotic imbalance created the driving force for a stochastic water flow from the pure-water compartment across the CNT membranes into the salt-solution compartment. For a gradient created by a $\Delta C \approx 6$ mol per liter NaCl solution, the rate of water flow per CNT was approximately $j = 5$ water molecules per nanosecond, corresponding to an osmotic permeability coefficient (112, 114) of approximately $p_f = j/\Delta C \approx 10^{-12}$ cm^3 s^{-1}, which is roughly a factor of ten larger than that measured for aquaporin AQP1 (115). Considering that single-file flow dominates in both the CNTs and AQP1, and that the constriction in AQP1 has similar dimensions, this order-of-magnitude agreement is not entirely surprising.

Having a smooth pore of low polarity appears to be a key factor for the fast flow rates seen in the simulations. As the water molecules pass through the pore, they do not form strong interactions with the pore, and therefore cannot transfer translational momentum to it. Correspondingly, the flow friction is very low. Indeed, wall friction is so low that the flow rate is nearly independent of the tube's length in the regime up to several nanometers probed by simulations (28). Instead, water flow is limited by molecular events associated with water entry into the tube and exit from it. Importantly, the resulting water flow rates are much larger than those predicted from the Hagen-Poiseuille formula of macroscopic hydrodynamics.

Recent experiments for fluid flow through membrane-embedded CNTs broadly confirmed the simulation results of fast water flow through CNTs (30, 31, 116, 117).

With diameters of 1–2 nm, the pores in Holt et al.'s (31) experiments were only slightly wider than in the simulations (21, 28). Both the experiments of Holt et al. (31) and Majumder et al. (30) gave water flow rates that exceeded the Hagen-Poiseuille values by factors of ∼1000 and more.

Ion Transport

Ions are well hydrated in aqueous solutions, with the favorable enthalpy owing to ion-water interactions. The partitioning of ions into a narrow CNT requires them to shed a significant fraction of their hydration shell water (118), thereby increasing both the barrier for partitioning as well as the free energy of transfer into the interior (119). Indeed, we found a membrane comprising (6,6) CNTs to be impermeable to sodium and chloride ions, and therefore it could be used to pump water osmotically (27, 28). High barriers for ion permeation were also observed by Sansom and collaborators (120).

Interestingly, the interior of somewhat larger CNTs can accommodate sufficient water molecules for it to retain at least some of its ability to dissolve ions. Simulations of ion permeation through CNT membranes (27) showed that pores with an effective, water-accessible diameter of ∼1 nm were permeable to sodium ions. In those pores, the ions retained their first hydration shell, resulting in a free-energy barrier for translocation of only a few $k_B T$. Dzubiella and colleagues' (63, 65) simulations showed further that local electric fields can affect the ion permeation. Remarkably, the nonpolar pores in the gating region of potassium channels have dimensions of ∼0.4 and ∼1.2 nm in the closed and open states, respectively (26, 121). The simulations (27, 120) suggest that this rather modest change is sufficient to switch between states blocking and permitting ion passage, respectively.

Proton Conduction

The quasi-1D hydrogen-bonded wires of water molecules formed inside narrow CNTs are excellent conductors of protons. Simulations on quantum-mechanical energy surfaces from density-functional theory and empirical-valence bond approaches showed that the proton mobility along those wires exceeds that in bulk water by more than an order of magnitude (36–39). These results are consistent with earlier classical studies (122).

In the quasi-1D system, the conduction of an excess proton is well described by Grotthuss-type (123) diffusion of a charge defect (36, 37). In a 1D chain, the motion of the defect requires only relatively small and local rearrangements (**Supplemental Figure 1**, top panel; follow the Supplemental Material link from the Annual Reviews home page at **http://www.annualreviews.org**). In contrast, proton motion in bulk water is strongly coupled to orientational changes in the second solvation shell (124) and beyond (125, 126), making it effectively slower (**Supplemental Figure 1**, bottom panel).

To complete the proton transfer along a 1D water chain in a nanopore, the dipole orientation of the water molecules has to revert back to its original direction (122). That second step transfers approximately 40% of the effective charge, on top of the

60% associated with the motion of the charge defect (36). Simulations show that the dipole flip is fast, occurring through the diffusive motion of a hydrogen-bonding defect (127, 128), and does not limit the overall proton transfer rate (36).

High conductivity requires not only fast charge mobility but also a large charge concentration. For CNT membranes in contact with bulk water, simulations suggest that the desolvation penalty for protons is large (36). The concentration of protons in the pores thus remains low, reminiscent of charge exclusion in biological water pores (107–111). The current density estimated from simulations (36) is approximately two orders of magnitude below that of polymer electrolyte membranes. However, one may use the proton concentration's sensitivity to the interaction energy to reach the currents required in fuel cells, taking advantage of the low electro-osmotic drag (36).

Methane/Solute Transport

Researchers have extensively studied the transport of methane and other gases through CNTs (129). Here we focus on molecular flows in condensed liquid phases. The uniformly nonpolar interior space of CNTs can accommodate not only water but also other molecular solutes dissolved in the aqueous phase.

In simulations of a CNT in methane-water solutions, methanes sampled the space vicinal to the CNT rim, breaking the single-file hydrogen-bonded water wire over nanosecond timescales and partitioning into the tube (33). Other methanes rapidly followed and filled the tube over subnanosecond timescales. Preliminary studies of CNTs with larger interior diameters, and with other test solutes (e.g., octane, methanol), also showed selective partitioning.

As shown elsewhere (33), the partitioning of nonpolar solutes into CNTs is highly favorable. As a result, once a CNT is filled with methanes, water molecules rarely enter the tube, whereas methanes from outside do exchange with those inside, by entering through one end and pushing a methane through the other (**Figure 1**). Several of such concerted events lead to the translocation of a methane molecule through the tube. Thus, the large thermodynamic driving force for filling leads to highly selective transport. Interestingly, first passage time distributions obtained directly from MD simulations, or by fitting a stochastic model to the simulation data, indicate the net rate of methane transport to be ~11 molecules per nanosecond per CNT for a concentration gradient of 1 mol per liter, exceeding that of water (28).

Studies of methane and water partitioning and transport highlight the underlying principle that selective partitioning leads to selective transport. This is likely relevant to biological channels designed to transport low-concentration solutes across physical barriers, such as membranes. For example, both glycerol (106) and potassium channels (121) have distinct binding sites that help partition their substrate as a prerequisite to transport.

Nucleic Acids and Peptides

With their weakly polar character, CNTs in water interact strongly not only with dissolved nonpolar molecules such as methane (33), but also with molecules with

amphiphilic character such as nucleic acids (34) and peptides (130). Simulations showed that under the influence of electric fields, small single-stranded RNA molecules passed through CNT membranes with pore diameters of ~1.4 nm. Differences in the amino acid sequence of the RNA affected the translocation rate through steric effects and the strength of hydrophobic interactions. After multiple translocations through a series of membranes, those differences led to the gradual separation of RNA molecules with different base sequences (34), suggesting possible applications in nanoscale molecular separation. Covalent modifications (131, 132) of the CNTs should further enhance the specificity of such devices.

CONCLUSIONS AND FUTURE DIRECTIONS

The work reviewed here is intended in part to provide a framework for thinking about thermodynamic, structural, and kinetic aspects of water under various nanoscopic confinements, as well as molecular partitioning and transport of water and solutes through microscopic channels. It reflects on an exciting area of research of fluids properties and transport at the small-systems level (133). The specific examples highlight nanoscopic systems as distinct from homogeneous bulk systems, and point to potential technological applications beyond the obvious academic interest.

The shape of the cavity space inside CNTs or fullerenes and the uniform graphitic chemistry with its remarkable molecular smoothness (in the absence of defects) have important consequences on the thermodynamic and structural properties of fluids, especially water, that fill them. The enthalpy of water transfer into the pore typically dominates the free energy of transfer, indicating the importance of water-water hydrogen bonds and water-cavity van der Waals interactions (22, 42). As a consequence, a rich variety of water structures emerge, ranging from single-file hydrogen-bonded wires in CNTs with small diameters (21) over various *N* body clusters inside fullerenes (22) to several new phases of quasi-1D ice in CNTs of diameters in the range of 1–1.5 nm (86, 89). In most cases, the observed structures are unique to nanoscopic systems and difficult or impossible to stabilize in the absence of confinement. Nanoscopic confinement also affects thermodynamic properties and phase behavior. The presence of a solid-liquid critical point for ice-water systems inside CNTs (86), a shift to lower temperatures in the anomalous thermodynamic properties of water in slit-pore geometries (134, 135), and the formation of bilayer ice between hydrophobic plates (92) are a few representative examples.

Studies of nanoscopically confined water have already led to new insights into the molecular function of proteins (35, 43). The fast flow of water through CNTs (21, 28, 29) captures important aspects of the flow through aquaporins (107, 108). Drying and wetting of protein channels have been suggested as factors in channel gating (46, 136, 137). Changes in the redox or protonation state, or the structure of the protein, can control such drying. The transient uptake of water molecules, triggered by changes in the local structure and charge states in cytochrome P450 (24, 25) and bacteriorhodopsin (138, 139), is thought to mediate proton transfer. Indeed, simulations for model systems showed remarkably fast proton transfer rates along single-file chains of water (36–39, 122). These fast rates, combined with the collective

dipolar orientation of the water wires, may be central to the function of cytochrome *c* oxidase, the proton pump powering aerobic life (140). The unidirectional transfer of protons along the water wire, with its orientation controlled by the redox state of the enzyme through electric fields (42), suggests that water molecules act as a diode for proton-transfer reactions.

Properties of molecular flows differ significantly from those of macroscopic hydrodynamic flows. Even in an osmotically driven flow that follows the gradient in free energy, instantaneous flow is stochastic in nature and can be described well by a 1D continuous-time random-walk model (28). The smooth hydrophobic walls of the CNT offer little hydrodynamic friction, and surprisingly high flow rates can be achieved, indicating significant slip at the wall (30, 31, 116, 117). How the stochastic nature of the flow is coarse grained with increasing tube diameter to eventually overlap with continuum hydrodynamics expectations is not entirely understood and presents an interesting direction for future research.

The simulation work described here focuses on the partitioning of water (and other molecules) into simple model nanoscopic systems of different shapes—cylindrical, spherical, and slit-pore-like. These geometries already have parallels in biomolecular systems that self-assemble and perform specific functions (43, 104, 105). With the advent of experimental methods of CNT synthesis (141, 142) and functionalization (131, 132, 143), and an improved understanding of micro- and nanofluidics (144), it is not difficult to imagine the development of nanofluidic networks to transport small quantities of fluid molecules from one location to another, mimicking at the smallest scale the network of pumps, pipes, and valves used in our everyday world to transport fluids. Fundamentally interesting results on filling/emptying binary transitions in CNTs (21) suggest that gating or control of fluid flow may be possible *via* several strategies, including altering the difference in the chemical potential of water inside and outside the tube. The possibility of the functionalization of CNT rims using short polymers or peptides (131, 132) may allow one to design molecular valves (145) that are selective to certain molecules and open or close in response to external stimuli, such as pH, salt or osmolyte concentration, hydrostatic pressure, and light. Simulations of fluid flow through a Y-junction CNT (146) have been reported. Junctions of CNTs have been made experimentally (147) by welding CNTs together (148). If the internal pores of Y- or T-shaped tubes can indeed be connected, such tubes would form ideal components in nanofluidic networks. Osmotic pumping of water through CNT membranes (28) or a fluid propeller made from a functionalized CNT (149) or electro-osmotic flow (32) may serve to drive fluid motion in such networks.

Simulations and recent experimental results demonstrating unexpectedly fast flow of water and other liquids through membranes containing CNTs (30, 31, 116, 117) suggest potential applications in a number of areas, including desalination, water purification, and molecular separations. Of course, numerous technological and fundamental hurdles need to be overcome before such applications truly can be realized. Technological hurdles revolve around the ability to synthesize nanoscopic components with precision and reproducibility, the chemical functionalization of the components, and the creation of such designs on a relatively large scale in an affordable manner.

SUMMARY POINTS

1. Water can fill nonpolar pores and cavities of nanoscopic dimensions, such as those in nanotubes and proteins, but the filling is highly sensitive to the effective pore polarity and solvent thermodynamic conditions.
2. Nonpolar pores form excellent low-friction conduits for the flow of water.
3. Protons move with high mobility along 1D water wires that form inside narrow CNTs.
4. Nonpolar cavities, including open-cage fullerenes, provide a means to study small and otherwise unstable hydrogen-bonded water clusters.
5. Proteins appear to exploit the unusual properties of confined water—e.g., the sensitivity of drying transitions to the effective polarity or fast proton transfer along 1D water wires—in their biological function.
6. The partitioning of water and other solutes into nanotubes and the low-friction flow through nanotubes open the possibility of designing nanofluidic devices in the future.

DISCLOSURE STATEMENT

The authors are not aware of any biases that might be perceived as affecting the objectivity of this review.

ACKNOWLEDGMENTS

J.C.R. acknowledges support from the National Science Foundation (grants CHE 0549187 and CHE 9961336). S.G. acknowledges financial support from the National Science Foundation (CAREER CTS-0134023 and NSEC DMR-0117792) and ACS-PRF grants. G.H. was supported by the Intramural Research Program of the NIH, NIDDK.

LITERATURE CITED

1. Wolfenden R, Radzicka A. 1994. On the probability of finding a water molecule in a nonpolar cavity. *Science* 265:936–37
2. Pratt LR, Pohorille A. 1992. Theory of hydrophobicity: transient cavities in molecular liquids. *Proc. Natl. Acad. Sci. USA* 89:2995–99
3. Eriksson AE, Baase WA, Zhang XJ, Heinz DW, Blaber M, et al. 1992. Response of a protein structure to cavity-creating mutations and its relation to the hydrophobic effect. *Science* 255:178–83
4. Ernst JA, Clubb RT, Zhou HX, Gronenborn AM, Clore GM. 1995. Demonstration of positionally disordered water within a protein hydrophobic cavity by NMR. *Science* 267:1813–17

5. Otting G, Liepinsh E, Halle B, Frey U. 1997. NMR identification of hydrophobic cavities with low water occupancies in protein structures using small gas molecules. *Nat. Struct. Biol.* 4:396–404
6. Yu B, Blaber M, Gronenborn AM, Clore GM, Caspar DLD. 1999. Disordered water within a hydrophobic protein cavity visualized by X-ray crystallography. *Proc. Natl. Acad. Sci. USA* 96:103–8
7. Dwyer JJ, Gittis AG, Karp DA, Lattman EE, Spencer DS, et al. 2000. High apparent dielectric constants in the interior of a protein reflect water penetration. *Biophys. J.* 79:1610–20
8. Quillin ML, Wingfield PT, Matthews BW. 2006. Determination of solvent content in cavities in Il-1β using experimentally phased electron density. *Proc. Natl. Acad. Sci. USA* 103:19749–53
9. Collins MD, Hummer G, Quillin ML, Matthews BW, Gruner SM. 2005. Cooperative water filling of a nonpolar protein cavity observed by high-pressure crystallography and simulation. *Proc. Natl. Acad. Sci. USA* 102:16668–71
10. Hummer G, Garde S, García AE, Paulaitis ME, Pratt LR. 1998. The pressure dependence of hydrophobic interactions is consistent with the observed pressure denaturation of proteins. *Proc. Natl. Acad. Sci. USA* 95:1552–55
11. García AE, Hummer G. 2000. Water penetration and escape in proteins. *Proteins Struct. Funct. Genet.* 38:261–72
12. Levy Y, Onuchic JN. 2006. Water mediation in protein folding and molecular recognition. *Annu. Rev. Biophys. Biomol. Struct.* 35:389–415
13. Petrone PM, García AE. 2004. MHC-peptide binding is assisted by bound water molecules. *J. Mol. Biol.* 338:419–35
14. Stillinger FH. 1973. Structure in aqueous solutions of nonpolar solutes from the standpoint of scaled-particle theory. *J. Solut. Chem.* 2:141–58
15. Lum K, Chandler D, Weeks JD. 1999. Hydrophobicity at small and large length scales. *J. Phys. Chem. B* 103:4570–77
16. Huang DM, Geissler PL, Chandler D. 2001. Scaling of hydrophobic solvation free energies. *J. Phys. Chem. B* 105:6704–9
17. Rajamani S, Truskett TM, Garde S. 2005. Hydrophobic hydration from small to large lengthscales: understanding and manipulating the crossover. *Proc. Natl. Acad. Sci. USA* 102:9475–80
18. Chandler D. 2005. Interfaces and the driving force of hydrophobic assembly. *Nature* 437:640–47
19. Hummer G, Garde S. 1998. Cavity expulsion and weak dewetting of hydrophobic solutes in water. *Phys. Rev. Lett.* 80:4193–96
20. Wallqvist A, Berne BJ. 1995. Computer simulation of hydrophobic hydration forces on stacked plates at short range. *J. Phys. Chem.* 99:2893–99
21. Hummer G, Rasaiah JC, Noworyta PJ. 2001. Water conduction through the hydrophobic channel of a carbon nanotube. *Nature* 414:188–90
22. Vaitheeswaran S, Yin H, Rasaiah JC, Hummer G. 2004. Water clusters in nonpolar cavities. *Proc. Natl. Acad. Sci. USA* 101:17002–5
23. Wikström M. 1998. Proton translocation by bacteriorhodopsin and heme-copper oxidases. *Curr. Opin. Struct. Biol.* 8:480–88

24. Schlichting I, Berendzen J, Chu K, Stock AM, Maves SA, et al. 2000. The catalytic pathway of cytochrome P450cam at atomic resolution. *Science* 287:1615–22
25. Taraphder S, Hummer G. 2003. Protein dynamics and hydration in proton transfer pathways: results for cytochrome P450cam. *J. Am. Chem. Soc.* 125:3931–40
26. Jiang Y, Lee A, Chen J, Cadene M, Chait BT, MacKinnon R. 2002. The open pore conformation of potassium channels. *Nature* 417:523–26
27. Peter C, Hummer G. 2005. Ion transport through membrane-spanning nanopores studied by molecular dynamics simulations and continuum electrostatics calculations. *Biophys. J.* 89:2222–34
28. Kalra A, Garde S, Hummer G. 2003. Osmotic water transport through carbon nanotube membranes. *Proc. Natl. Acad. Sci. USA* 100:10175–80
29. Berezhkovskii A, Hummer G. 2002. Single-file transport of water molecules through a carbon nanotube. *Phys. Rev. Lett.* 89:064503
30. Majumder M, Chopra N, Andrews R, Hinds BJ. 2005. Nanoscale hydrodynamics enhanced flow in carbon nanotubes. *Nature* 438:44
31. Holt JK, Park HG, Wang YM, Stadermann M, Artyukhin AB, et al. 2006. Fast mass transport through sub-2-nm carbon nanotubes. *Science* 312:1034–37
32. Miller SA, Young VY, Martin CR. 2001. Electroosmotic flow in template-prepared carbon nanotube membranes. *J. Am. Chem. Soc.* 123:12335–42
33. Kalra A, Hummer G, Garde S. 2004. Methane partitioning and transport in hydrated carbon nanotubes. *J. Phys. Chem. B* 108:544–49
34. Yeh IC, Hummer G. 2004. Nucleic acid transport through carbon nanotube membranes. *Proc. Natl. Acad. Sci. USA* 101:12171–82
35. Hummer G. 2007. Water, proton, and ion transport: from nanotubes to proteins. *Mol. Phys.* 105:201–7
36. Dellago C, Hummer G. 2006. Kinetics and mechanism of proton transport across membrane nanopores. *Phys. Rev. Lett.* 97:245901
37. Dellago C, Naor MM, Hummer G. 2003. Proton transport through water-filled carbon nanotubes. *Phys. Rev. Lett.* 90:105902
38. Hassan SA, Hummer G, Lee YS. 2006. Effects of electric fields on proton transport through water chains. *J. Chem. Phys.* 124:204510
39. Brewer ML, Schmitt UW, Voth GA. 2001. The formation and dynamics of proton wires in channel environments. *Biophys. J.* 80:1691–702
40. Kreuer KD, Paddison SJ, Spohr E, Schuster M. 2004. Transport in proton conductors for fuel-cell applications simulations elementary reactions and phenomenology. *Chem. Rev.* 104:4637–78
41. Bennett CH. 1976. Efficient estimation of free energy differences from Monte Carlo data. *J. Comput. Phys.* 22:245–68
42. Vaitheeswaran S, Rasaiah JC, Hummer G. 2004. Electric field and temperature effects on water in carbon nanotubes. *J. Chem. Phys.* 121:7955–65
42a. Waghe A. 2007. *Computer simulations of water and methanol in carbon nanotubes*. PhD thesis. Univ. Maine, Orono

43. Yin H, Hummer G, Rasaiah JC. 2007. Metastable water clusters in the nonpolar cavities of the thermostable protein tetrabrachion. *J. Am. Chem. Soc.* 129:7369–77
44. Maibaum L, Chandler D. 2003. A coarse-grained model of water confined in a hydrophobic tube. *J. Phys. Chem. B* 107:1189–93
45. Waghe A, Rasaiah JC, Hummer G. 2002. Filling and emptying kinetics of carbon nanotubes in water. *J. Chem. Phys.* 117:10789–95
46. Beckstein O, Biggin PC, Sansom MSP. 2001. A hydrophobic gating mechanism for nanopores. *J. Phys. Chem. B* 105:12902–5
47. Beckstein O, Sansom MSP. 2003. Liquid-vapor oscillations of water in hydrophobic nanopores. *Proc. Natl. Acad. Sci. USA* 100:7063–68
48. Choudhury N, Pettitt BM. 2005. On the mechanism of hydrophobic association of nanoscopic solutes. *J. Am. Chem. Soc.* 127:3556–67
49. Allen R, Melchionna S, Hansen JP. 2002. Intermittent permeation of cylindrical nanopores by water. *Phys. Rev. Lett.* 89:175502
50. Allen R, Hansen JP, Melchionna S. 2003. Molecular dynamics investigation of water permeation through nanopores. *J. Chem. Phys.* 119:3905–19
51. Brovchenko I, Paschek D, Geiger A. 2000. Gibbs ensemble simulation of water in spherical cavities. *J. Chem. Phys.* 113:5026–36
52. Leung K, Luzar A, Bratko D. 2003. Dynamics of capillary drying in water. *Phys. Rev. Lett.* 90:065502
53. Vaitheeswaran S, Yin H, Rasaiah JC. 2005. Water between plates in the presence of an electric field in an open system. *J. Phys. Chem. B* 109:6629–35
54. Ramachandran CE, Chempath S, Broadbelt LJ, Snurr RQ. 2006. Water adsorption in hydrophobic nanopores: Monte Carlo simulations of water in silicalite. *Micropor. Mesopor. Mater.* 90:293–98
55. Striolo A, Gubbins KE, Chialvo AA, Cummings PT. 2004. Simulated water adsorption isotherms in carbon nanopores. *Mol. Phys.* 102:243–51
56. Zhou RH, Huang XH, Margulis CJ, Berne BJ. 2004. Hydrophobic collapse in multidomain protein folding. *Science* 305:1605–9
57. Liu P, Huang XH, Zhou RH, Berne BJ. 2005. Observation of a dewetting transition in the collapse of the melittin tetramer. *Nature* 437:159–62
58. Giovambattista N, Debenedetti PG, Rossky PJ. 2007. Hydration behavior under confinement by nanoscale surfaces with patterned hydrophobicity and hydrophilicity. *J. Phys. Chem. C* 111:1323–32
59. Werder T, Walther JH, Jaffe RL, Halicioglu T, Koumoutsakos P. 2003. On the water-carbon interaction for use in molecular dynamics simulations of graphite and carbon nanotubes. *J. Phys. Chem. B* 107:1345–52
60. Collins MD, Quillin ML, Hummer G, Matthews BW, Gruner SM. 2007. Structural rigidity of a large cavity-containing protein revealed by high-pressure crystallography. *J. Mol. Biol.* 367:752–63
61. Dunitz JD. 1994. The entropic cost of bound water in crystals and biomolecules. *Science* 264:670
62. Denisov VP, Venu K, Peters J, Horlein HD, Halle B. 1997. Orientational disorder and entropy of water in protein cavities. *J. Phys. Chem. B* 101:9380–89

63. Dzubiella J, Allen RJ, Hansen JP. 2004. Electric field-controlled water permeation coupled to ion transport through a nanopore. *J. Chem. Phys.* 120:5001–4
64. Li JY, Gong XJ, Lu HJ, Li D, Fang HP, Zhou RH. 2007. Electrostatic gating of a nanometer water channel. *Proc. Natl. Acad. Sci. USA* 104:3687–92
65. Dzubiella J, Hansen JP. 2005. Electric-field-controlled water and ion permeation of a hydrophobic nanopore. *J. Chem. Phys.* 122:234706
66. Zimmerli U, Gonnet PG, Walther JH, Koumoutsakos P. 2005. Curvature induced *L*-defects in water conduction in carbon nanotubes. *Nano Lett.* 5:1017–22
67. Bratko D, Daub DD, Leung K, Luzar A. 2007. Effect of field direction on electrowetting in a nanopore. *J. Am. Chem. Soc.* 129:2504–10
68. Andreev S, Reichman D, Hummer G. 2005. Effect of flexibility on hydrophobic behavior of nanotube water channels. *J. Chem. Phys.* 123:194502
69. Damjanović A, Schlessman JL, Fitch CA, García AE, García-Moreno E. 2007. Role of flexibility and polarity as determinants of the hydration of internal cavities and pockets in proteins. *Biophys. J.* 93:2791–804
70. Lee CY, McCammon JA, Rossky PJ. 1984. The structure of liquid water at an extended hydrophobic surface. *J. Chem. Phys.* 80:4448–55
71. Granick S. 1991. Motions and relaxations of confined liquids. *Science* 253:1374–79
72. Gordillo MC, Martí J. 2000. Hydrogen bond structure of liquid water confined in nanotubes. *Chem. Phys. Lett.* 329:341–45
73. Walther JH, Jaffe R, Halicioglu T, Koumoutsakos P. 2001. Carbon nanotubes in water: structural characteristics and energetics. *J. Phys. Chem. B* 105:9980–87
74. Martí J, Gordillo MC. 2001. Temperature effects on the static and dynamic properties of liquid water inside nanotubes. *Phys. Rev. E* 64:021504
75. Iwamatsu S, Uozaki T, Kobayashi K, Re SY, Nagase S, Murata S. 2004. A bowl-shaped fullerene encapsulates a water into the cage. *J. Am. Chem. Soc.* 126:2668–69
76. Keutsch FN, Saykally RJ. 2001. Water clusters: untangling the mysteries of the liquid one molecule at a time. *Proc. Natl. Acad. Sci. USA* 98:10533–40
77. Ramachandran CN, Sathyamurthy N. 2005. Water clusters in a confined nonpolar environment. *Chem. Phys. Lett.* 410:348–51
78. Gogotsi Y, Libera JA, Guvenc-Yazicioglu A, Megaridis CM. 2001. In situ multiphase fluid experiments in hydrothermal carbon nanotubes. *Appl. Phys. Lett.* 79:1021–23
79. Maniwa Y, Kataura H, Abe M, Udaka A, Suzuki S, et al. 2005. Ordered water inside carbon nanotubes: formation of pentagonal to octagonal ice nanotubes. *Chem. Phys. Lett.* 401:534–38
80. Kolesnikov A, Zanotti J, Loong C. 2004. Anomalously soft dynamics of water in a nanotube: a revelation of nanoscale confinement. *Phys. Rev. Lett.* 93:035503
81. Byl O, Liu JC, Wang Y, Yim WL, Johnson JK, Yates JT. 2006. Unusual hydrogen bonding in water-filled carbon nanotubes. *J. Am. Chem. Soc.* 128:12090–97
82. Sekhaneh W, Kotecha M, Dettlaff-Weglikowska U, Veeman WS. 2006. High resolution NMR of water absorbed in single-wall carbon nanotubes. *Chem. Phys. Lett.* 428:143–47

83. Matsuda K, Hibi T, Kadowaki H, Kataura H, Maniwa Y. 2006. Water dynamics inside single-wall carbon nanotubes: NMR observations. *Phys. Rev. B* 74:073415
84. Mao SH, Kleinhammes A, Wu Y. 2006. NMR study of water adsorption in single-walled carbon nanotubes. *Chem. Phys. Lett.* 421:513–17
85. Dujardin E, Ebbesen TW, Hiura H, Tanigaki K. 1994. Capillarity and wetting of carbon nanotubes. *Science* 265:1850–52
86. Koga K, Gao GT, Tanaka H, Zeng XC. 2001. Formation of ordered ice nanotubes inside carbon nanotubes. *Nature* 412:802–5
87. Bai J, Su CR, Parra RD, Zeng XC, Tanaka H, et al. 2003. Ab initio studies of quasi-one-dimensional pentagon and hexagon ice nanotubes. *J. Chem. Phys.* 118:3913–16
88. Koga K, Gao GT, Tanaka H, Zeng XC. 2002. How does water freeze inside carbon nanotubes? *Phys. A* 314:462–69
89. Bai JE, Wang J, Zeng XC. 2006. Multiwalled ice helixes and ice nanotubes. *Proc. Natl. Acad. Sci. USA* 103:19664–67
90. Meyer RR, Sloan J, Dunin-Borkowski RE, Kirkland AI, Novotny MC, et al. 2000. Discrete atom imaging of one-dimensional crystals formed within single-walled carbon nanotubes. *Science* 289:1324–26
91. Wilson M, Madden PA. 2001. Growth of ionic crystals in carbon nanotubes. *J. Am. Chem. Soc.* 123:2101–2
92. Giovambattista N, Rossky PJ, Debenedetti PG. 2006. Effect of pressure on the phase behavior and structure of water confined between nanoscale hydrophobic and hydrophilic plates. *Phys. Rev. E* 73:041604
93. Buckle AM, Cramer P, Fersht AR. 1996. Structural and energetic responses to cavity-creating mutations in hydrophobic cores: observation of a buried water molecule and the hydrophilic nature of such hydrophobic cavities. *Biochemistry* 35:4298–305
94. Zhang L, Hermans J. 1996. Hydrophilicity of cavities in proteins. *Proteins Struct. Funct. Genet.* 24:433–38
95. Roux B, Nina M, Pomes R, Smith JC. 1996. Thermodynamic stability of water molecules in the bacteriorhodopsin proton channel: a molecular dynamics free energy perturbation study. *Biophys. J.* 71:670–81
96. Helms V, Wade RC. 1995. Thermodynamics of water mediating protein-ligand interactions in cytochrome P450cam: a molecular dynamics study. *Biophys. J.* 69:810–24
97. Olano LR, Rick SW. 2004. Hydration free energies and entropies for water in protein interiors. *J. Am. Chem. Soc.* 126:7991–8000
98. Riistama S, Hummer G, Puustinen A, Dyer RB, Woodruff WH, Wikström M. 1997. Bound water in the proton translocation mechanism of the haem-copper oxidases. *FEBS Lett.* 414:275–80
99. Beglov D, Roux B. 1997. An integral equation to describe the solvation of polar molecules in liquid water. *J. Phys. Chem. B* 101:7821–26
100. Stetefeld J, Jenny M, Schulthess T, Landwehr R, Engel J, Kammerer RA. 2000. Crystal structure of a naturally occurring parallel right-handed coiled coil tetramer. *Nat. Struct. Biol.* 7:772–76

101. Peters J, Baumeister W, Lupas A. 1996. Hyperthermostable surface layer protein tetrabrachion from the archaebacterium *Staphylothermus marinus*: evidence for the presence of a right-handed coiled coil derived from the primary structure. *J. Mol. Biol.* 257:1031–41
102. Buchete NV, Tycko R, Hummer G. 2005. Molecular dynamics simulations of Alzheimer's β-amyloid protofilaments. *J. Mol. Biol.* 353:804–21
103. Rohrig UF, Laio A, Tantalo N, Parrinello M, Petronzio R. 2006. Stability and structure of oligomers of the Alzheimer peptide $A\beta_{16-22}$: from the dimer to the 32-mer. *Biophys. J.* 91:3217–29
104. Murata K, Mitsuoka K, Hirai T, Walz T, Agre P, et al. 2000. Structural determinants of water permeation through aquaporin-1. *Nature* 407:599–605
105. Sui HX, Han BG, Lee JK, Walian P, Jap BK. 2001. Structural basis of water-specific transport through the AQP1 water channel. *Nature* 414:872–78
106. Fu DX, Libson A, Miercke LJW, Weitzman C, Nollert P, et al. 2000. Structure of a glycerol-conducting channel and the basis for its selectivity. *Science* 290:481–86
107. de Groot BL, Grubmüller H. 2001. Water permeation across biological membranes: mechanism and dynamics of aquaporin-1 and GlpF. *Science* 294:2353–57
108. Tajkhorshid E, Nollert P, Jensen MO, Miercke LJW, O'Connell J, et al. 2002. Control of the selectivity of the aquaporin water channel family by global orientational tuning. *Science* 296:525–30
109. Chakrabarti N, Tajkhorshid E, Roux B, Pomès R. 2004. Molecular basis of proton blockage in aquaporins. *Structure* 12:65–74
110. Chen HN, Ilan B, Wu YJ, Zhu FQ, Schulten K, Voth GA. 2007. Charge delocalization in proton channels, I: the aquaporin channels and proton blockage. *Biophys. J.* 92:46–60
111. Burykin A, Warshel A. 2004. On the origin of the electrostatic barrier for proton transport in aquaporin. *FEBS Lett.* 570:41–46
112. Zhu FQ, Tajkhorshid E, Schulten K. 2002. Pressure-induced water transport in membrane channels studied by molecular dynamics. *Biophys. J.* 83:154–60
113. Murad S, Powles JG. 1993. A computer simulation of the classic experiment on osmosis and osmotic pressure. *J. Chem. Phys.* 99:7271–72
114. Finkelstein A. 1987. *Water Movement Through Lipid Bilayers, Pores, and Plasma Membranes*. New York: Wiley
115. Zeidel ML, Ambudkar SV, Smith BL, Agre P. 1992. Reconstitution of functional water channels in liposomes containing purified red-cell CHIP28 protein. *Biochemistry* 31:7436–40
116. Srivastava A, Srivastava ON, Talapatra S, Vajtai R, Ajayan PM. 2004. Carbon nanotube filters. *Nat. Mater.* 3:610–14
117. Casavant MJ, Walters DA, Schmidt JJ, Smalley RE. 2003. Neat macroscopic membranes of aligned carbon nanotubes. *J. Appl. Phys.* 93:2153–56
118. Lynden-Bell RM, Rasaiah JC. 1996. Mobility and solvation of ions in channels. *J. Chem. Phys.* 105:9266–80
119. Yang L, Garde S. 2007. Modeling the selective partitioning of cations into negatively charged nanopores in water. *J. Chem. Phys.* 126:084706

120. Beckstein O, Tai K, Sansom MSP. 2004. Not ions alone: barriers to ion permeation in nanopores and channels. *J. Am. Chem. Soc.* 126:14694–95
121. Zhou Y, Morais-Cabral JH, Kaufman A, MacKinnon R. 2001. Chemistry of ion coordination and hydration revealed by a K^+ channel-Fab complex at 2.0 Å resolution. *Nature* 414:43–48
122. Pomès R, Roux B. 1998. Free energy profiles for H^+ conduction along hydrogen-bonded chains of water molecules. *Biophys. J.* 75:33–40
123. de Grotthuss CJT. 1806. Sur la décomposition de l'eau et des corps qu'elle tient en dissolution à l'aide de l'électricité galvanique. *Ann. Chim.* 58:54–74
124. Agmon N. 1995. The Grotthuss mechanism. *Chem. Phys. Lett.* 244:456–62
125. Geissler PL, Dellago C, Chandler D, Hutter J, Parrinello M. 2001. Autoionization in liquid water. *Science* 291:2121–24
126. Marx D, Tuckerman ME, Hutter J, Parrinello M. 1999. The nature of the hydrated excess proton in water. *Nature* 397:601–4
127. Zhu FQ, Schulten K. 2003. Water and proton conduction through carbon nanotubes as models for biological channels. *Biophys. J.* 85:236–44
128. Best RB, Hummer G. 2005. Reaction coordinates and rates from transition paths. *Proc. Natl. Acad. Sci. USA* 102:6732–37
129. Skoulidas AI, Ackerman DM, Johnson JK, Sholl DS. 2002. Rapid transport of gases in carbon nanotubes. *Phys. Rev. Lett.* 89:185901
130. Sorin EJ, Pande VS. 2006. Nanotube confinement denatures protein helices. *J. Am. Chem. Soc.* 128:6316–17
131. Wong SS, Joselevich E, Woolley AT, Cheung CL, Lieber CM. 1998. Covalently functionalized nanotubes as nanometre-sized probes in chemistry and biology. *Nature* 394:52–55
132. Williams KA, Veenhuizen PTM, de la Torre BG, Eritja R, Dekker C. 2002. Carbon nanotubes with DNA recognition. *Nature* 420:761
133. Hill TL. 2001. Perspective: nanothermodynamics. *Nano Lett.* 1:111–12
134. Kumar P, Buldyrev SV, Starr FW, Giovambattista N, Stanley HE. 2005. Thermodynamics, structure, and dynamics of water confined between hydrophobic plates. *Phys. Rev. E.* 72:051503
135. Truskett TM, Debenedetti PG, Torquato S. 2001. Thermodynamic implications of confinement for a waterlike fluid. *J. Chem. Phys.* 114:2401–18
136. Sotomayor M, Schulten K. 2004. Molecular dynamics study of gating in the mechanosensitive channel of small conductance MscS. *Biophys. J.* 87:3050–65
137. Anishkin A, Sukharev S. 2004. Water dynamics and dewetting transitions in the small mechanosensitive channel MscS. *Biophys. J.* 86:2883–95
138. Hummer G, Rasaiah JC, Noworyta JP. 2002. Water conduction through carbon nanotubes. *Tech. Proc. 2nd Int. Conf. Comput. Nanosci. Nanotechnol.*, ed. M Laudon, B Romanowicz, pp. 124–27. Cambridge, MA: Comput. Publ.
139. Schobert B, Brown LS, Lanyi JK. 2003. Crystallographic intermediates of structures of the M and N bacteriorhodopsin: assembly of a hydrogen-bonded chain of water molecules between Asp-96 and the retinal Schiff base. *J. Mol. Biol.* 330:553–70

140. Wikström M, Verkhovsky MI, Hummer G. 2003. Water-gated mechanism of proton translocation by cytochrome *c* oxidase. *Biochim. Biophys. Acta Bioenerg.* 1604:61–65
141. Ajayan PM, Tour JM. 2007. Materials science: nanotube composites. *Nature* 447:1066–68
142. Talapatra S, Kar S, Pal SK, Vajtai R, Ci L, et al. 2006. Direct growth of aligned carbon nanotubes on bulk metals. *Nat. Nanotechnol.* 1:112–16
143. Rege K, Raravikar NR, Kim DY, Schadler LS, Ajayan PM, Dordick JS. 2003. Enzyme–polymer–single walled carbon nanotube composites as biocatalytic films. *Nano Lett.* 3:829–32
144. Bocquet L, Barrat JL. 2007. Flow boundary conditions from nano- to micro-scales. *Soft Matter* 3:685–693
145. Maniwa Y, Matsuda K, Kyakuno H, Ogasawara S, Hibi T, et al. 2007. Water-filled single-wall carbon nanotubes as molecular nanovalves. *Nat. Mater.* 6:135–41
146. Park JH, Sinnott SB, Aluru NR. 2006. Ion separation using a Y-junction carbon nanotube. *Nanotechnology* 17:895–900
147. Satishkumar BC, Thomas PJ, Govindaraj A, Rao CNR. 2000. Y-junction carbon nanotubes. *Appl. Phys. Lett.* 77:2530–32
148. Yoon M, Han SW, Kim G, Lee SB, Berber S, et al. 2004. Zipper mechanism of nanotube fusion: theory and experiment. *Phys. Rev. Lett.* 92:075504
149. Wang B, Král P. 2007. Chemically tunable nanoscale propellers of liquids. *Phys. Rev. Lett.* 98:266102
150. Cicero G, Grossman JC, Schwegler E, Gygi F, Galli G. 2007. Water confined in nanotubes and between graphene sheets: a first principle study. *J. Am. Chem. Soc.* In press

Annual Review of
Physical Chemistry

Volume 59, 2008

Contents

Indexes

Errata

An online log of corrections to *Annual Review of Physical Chemistry* articles may be found at http://physchem.annualreviews.org/errata.shtml